

# Supporting Information

to

## Loop to Linear: Exploring the Impact of Corona Topology on the Properties of Self-Assembled Polymer Nanoparticles

*Haoxiang Zeng,<sup>1</sup> and Markus Müllner<sup>1,2\*</sup>*

<sup>1</sup>Key Centre for Polymers and Colloids, School of Chemistry, The University of Sydney, Sydney, NSW 2006, Australia;

<sup>2</sup>The University of Sydney Nano Institute (Sydney Nano), Sydney, NSW 2006, Australia.

Email correspondence to [markus.muellner@sydney.edu.au](mailto:markus.muellner@sydney.edu.au)

Experimental Procedures .....	2
Supplementary Results and Discussion.....	3
S1. Characterisation of Initiator and Polymers .....	3
S2. Drug Release Profile of Self-Assembled Polymer Nanoparticles .....	10
S3. EIS Experiment Set-up and Results .....	12
References .....	14

## Experimental Procedures

*Synthesis of 5-propargylether-2-nitrobenzyl bromoisobutyrate.* The UV-responsive ATRP initiator was synthesised according to the previously reported method,<sup>1</sup> as illustrated in Scheme 1(a). First, 5-hydroxy-2-nitrobenzyl alcohol (1000 mg, 5.9 mmol, 1 eq.) and K<sub>2</sub>CO<sub>3</sub> (2451 mg, 17.7 mmol, 3 eq.) were stirred in 15 ml DMF at 60 °C. Subsequently, propargyl bromide (538  $\mu$ l, 7.1 mmol, 1.2 eq.) was added to the solution dropwise to start the nucleophilic substitution. The reaction mixture was left to stir at 60 °C for 24 hours. DMF was removed under reduced pressure. The product was then redissolved into ethyl acetate and washed with deionised water and brine for three times. The dried products (5-propargylether-2-nitrobenzyl alcohol) were characterised by <sup>1</sup>H NMR (**Figure S1**) and found pure enough to proceed to the next step. The yield was 87%.

5-propargylether-2-nitrobenzyl alcohol was then used to react with  $\alpha$ -bromoisobutyryl bromide to prepare 5-propargylether-2-nitrobenzyl bromoisobutyrate. Briefly, a solution of  $\alpha$ -bromoisobutyryl bromide (860  $\mu$ L, 6.95 mmol, 1.2 eq.) in dry THF (9 ml) was slowly added to a stirred mixture of 5-propargylether-2-nitrobenzyl alcohol (1200 mg, 5.80 mmol, 1 eq.) and dry Et<sub>3</sub>N (970  $\mu$ L, 6.95 mmol, 1.2 eq.) in dry THF (9 ml) at 0°C and under nitrogen. The mixture was then left to run at room temperature overnight, after which distilled water was slowly added to the solution to stop the reaction. The solvent was removed under reduced pressure, and the remaining solid was dissolved into CH<sub>2</sub>Cl<sub>2</sub> and washed with deionised water. The products from the organic phases were further purified by flash chromatography (eluent: petroleum benzene/ethyl acetate=9/1) and characterised by <sup>1</sup>H NMR (**Figure S2**). The fraction was collected and dried as an off-white solid with 75% yield.

## Supplementary Results and Discussion

### S1. Characterisation of Initiator and Polymers

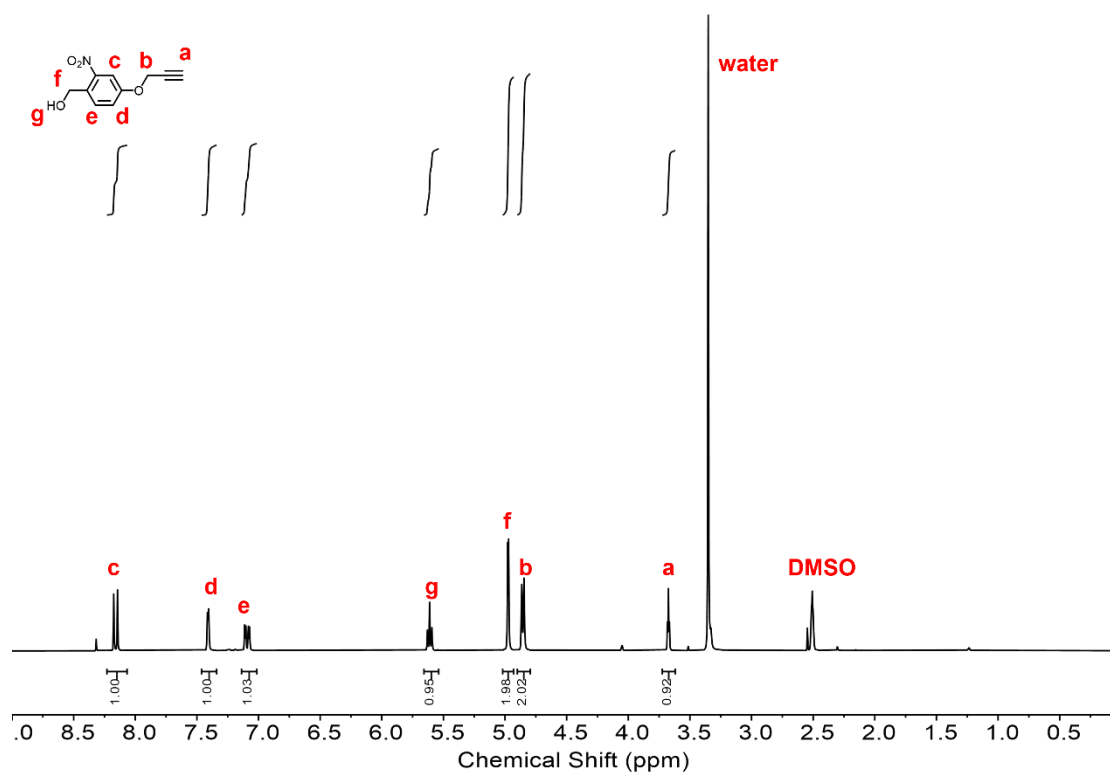


Figure S1. <sup>1</sup>H NMR of 5-propargylether-2-nitrobenzyl alcohol

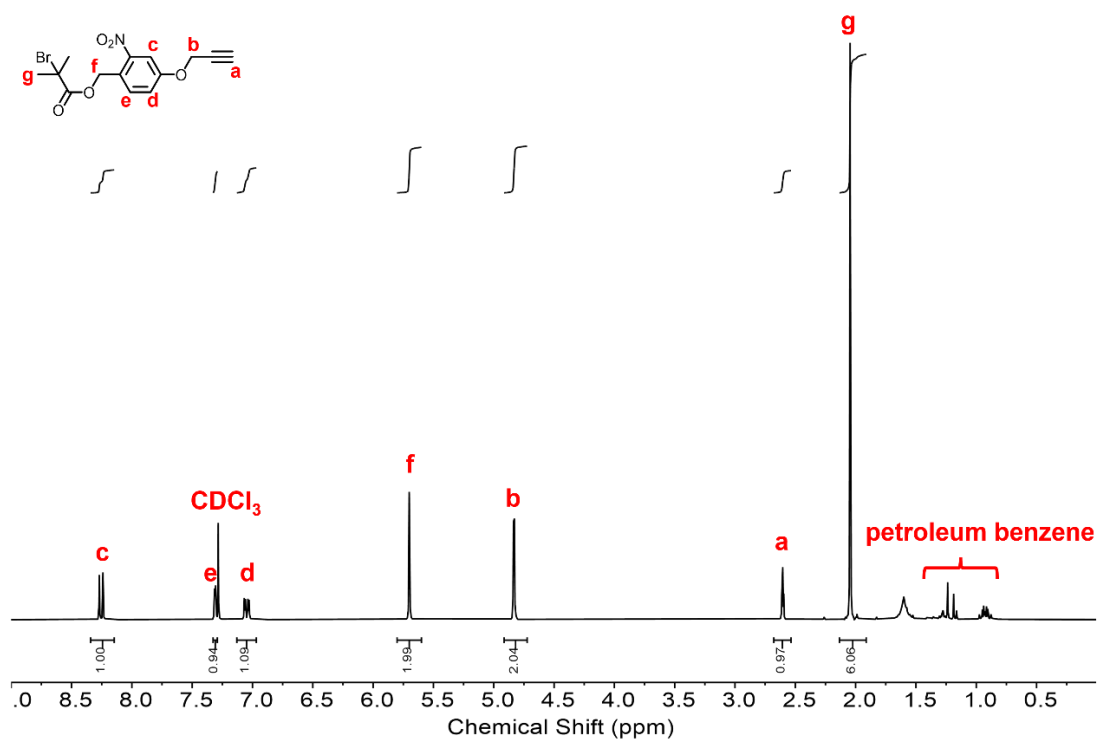
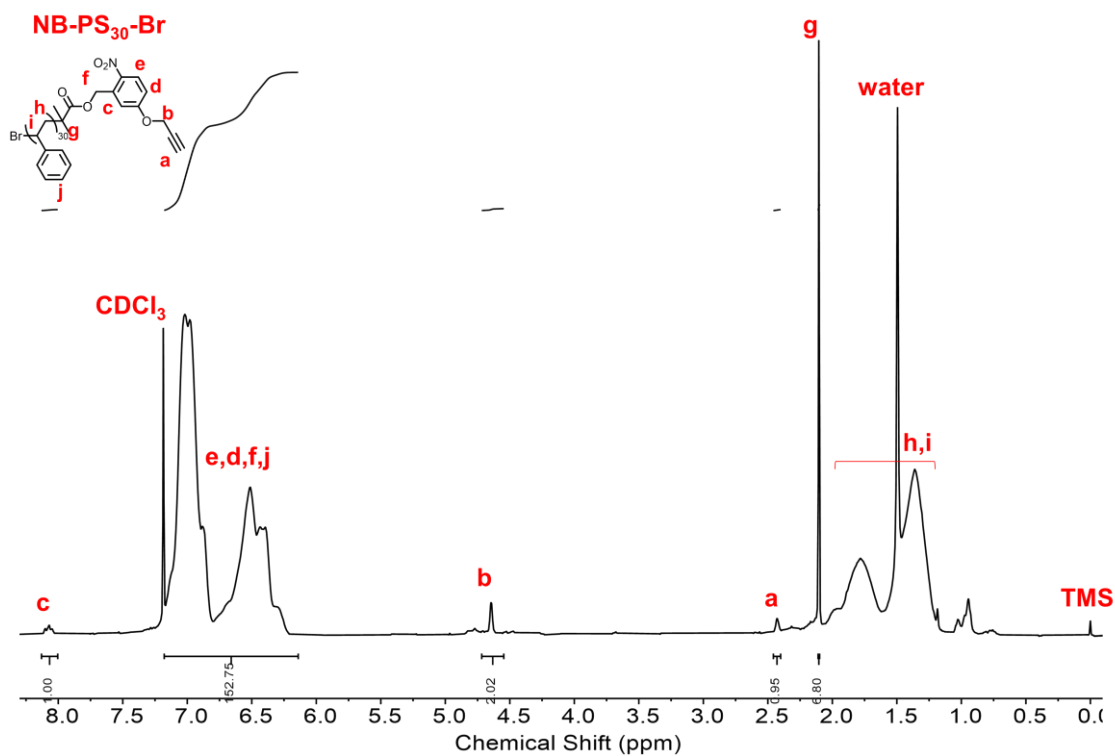
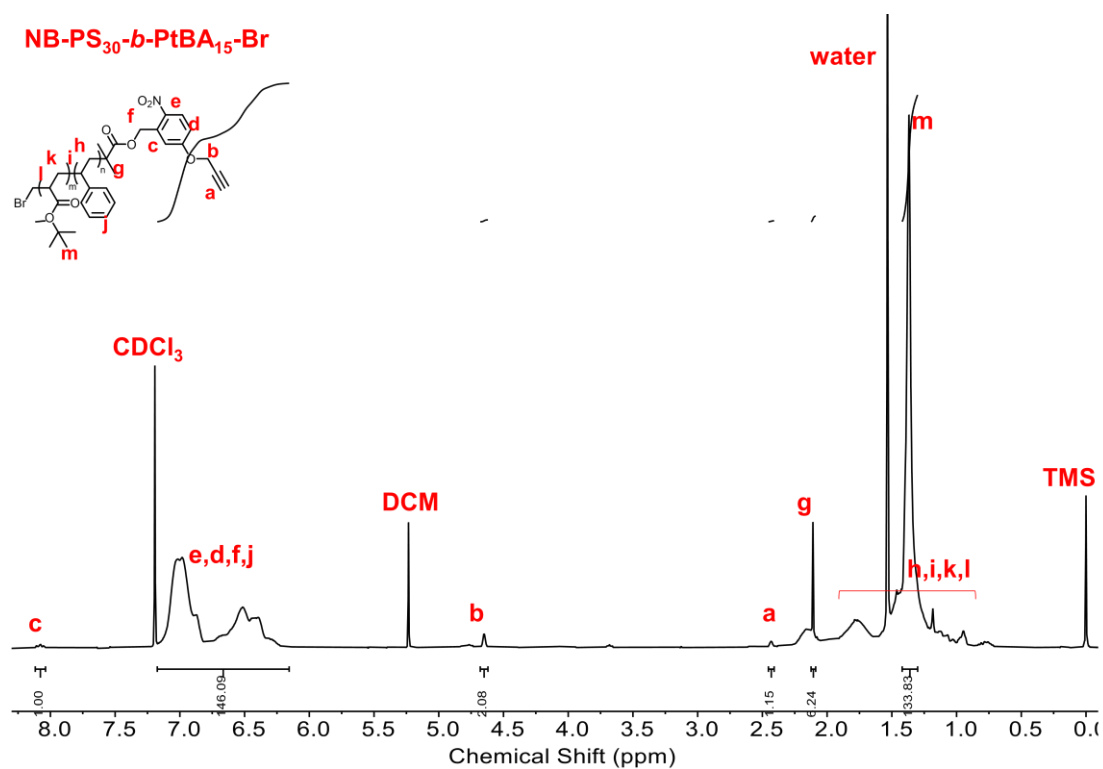


Figure S2. <sup>1</sup>H NMR of 5-propargylether-2-nitrobenzyl bromoisobutyrate



**Figure S3.** <sup>1</sup>H NMR of macroinitiator NB-PS<sub>30</sub>-Br



**Figure S4.** <sup>1</sup>H NMR of NB-PS<sub>30</sub>-b-PtBA<sub>15</sub>-Br

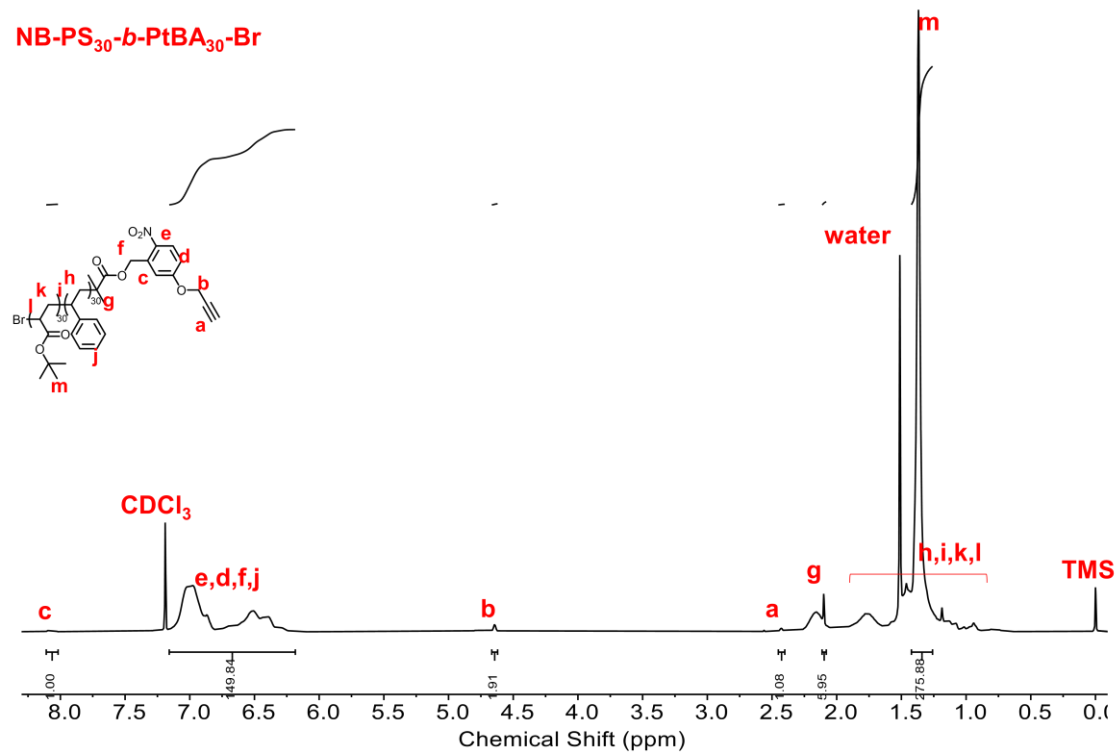


**Figure S5.** <sup>1</sup>H NMR of NB-PS<sub>30</sub>-*b*-PtBA<sub>30</sub>-Br

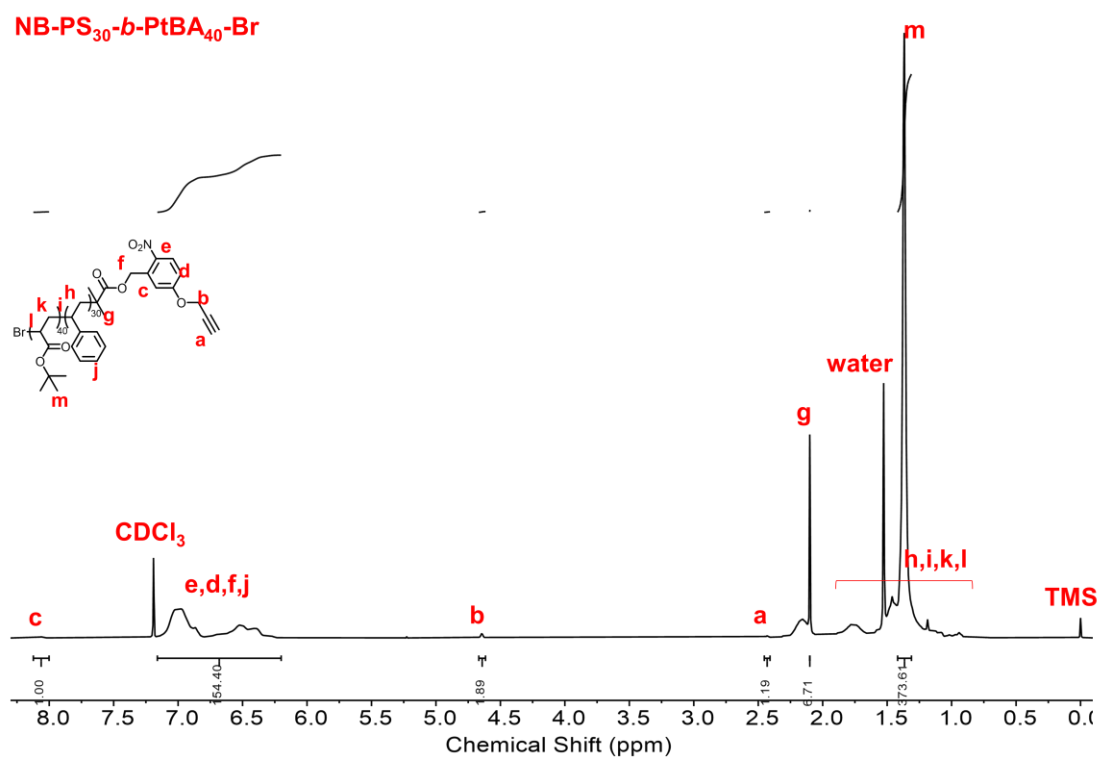


**Figure S6.** <sup>1</sup>H NMR of NB-PS<sub>30</sub>-*b*-PtBA<sub>40</sub>-Br

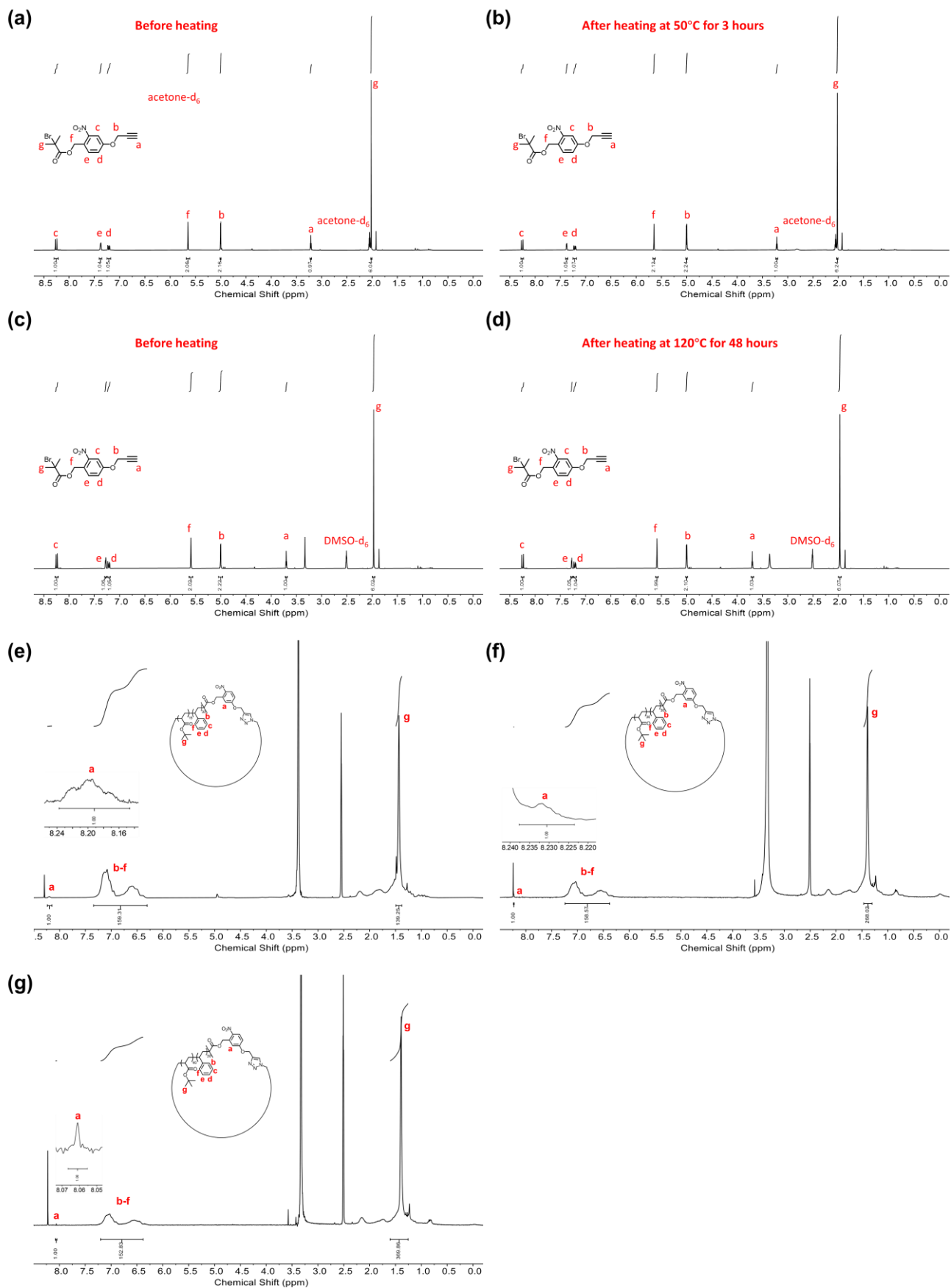


**Figure S7.** Thermal stability test of 5-propargylether-2-nitrobenzyl bromoisobutyrate in  $\text{Acetone-d}_6$  (a) before heating and (b) after heating to 50°C for 3 hours; in dried  $\text{DMSO-d}_6$  (c) before heating and

(d) after heating at 120°C for 48 hours; (e)-(g) Thermal stability test of polymers during cyclisation by using end group analysis.

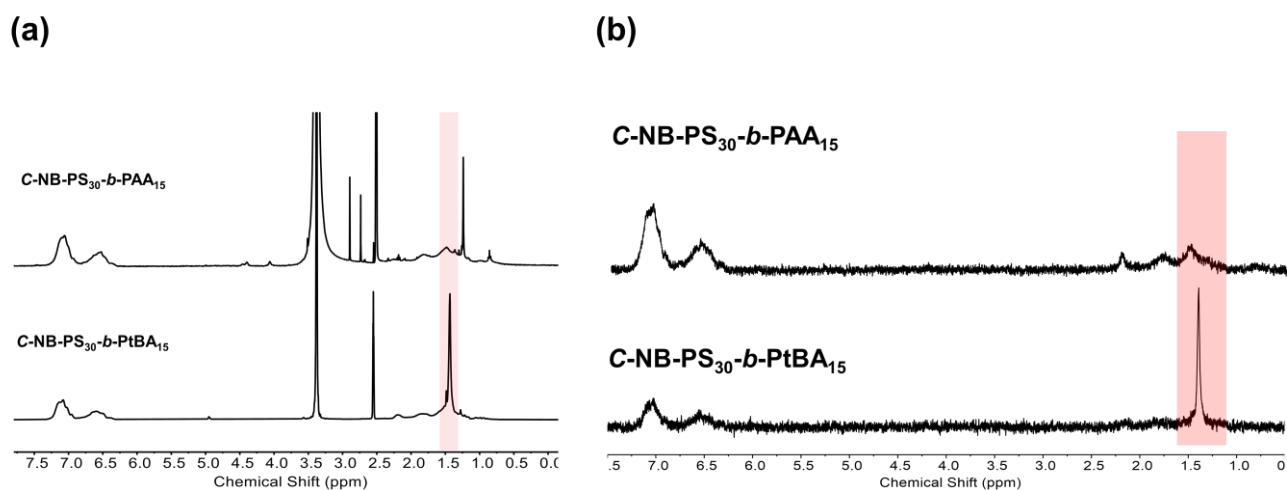


**Figure S8.** (a) <sup>1</sup>H NMR of C-NB-PS<sub>30</sub>-b-PtBA<sub>15</sub> before and after the deprotection. (b) <sup>1</sup>H NMR (solvent signals suppressed using DOSY) of C-NB-PS<sub>30</sub>-b-PtBA<sub>15</sub> before and after the deprotection.

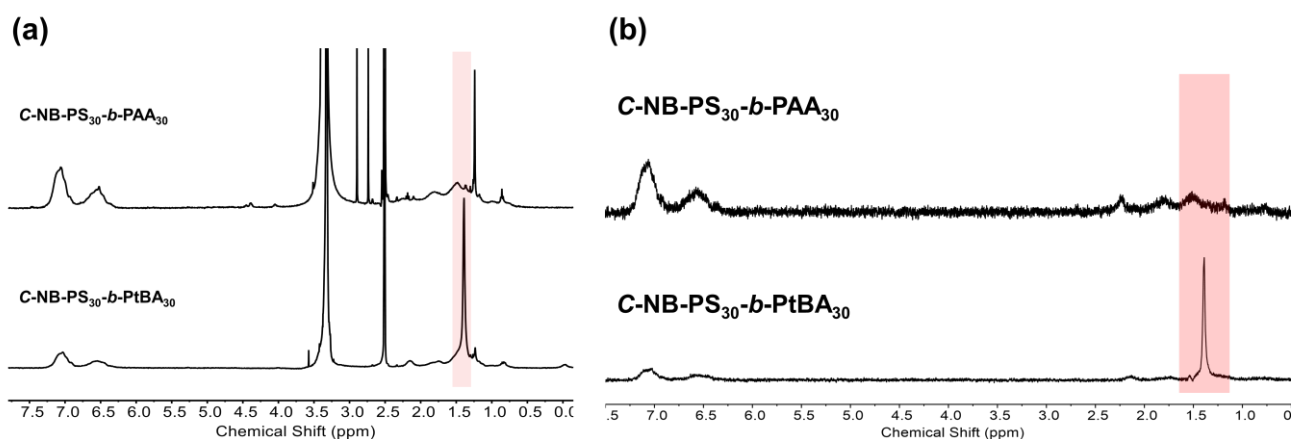


**Figure S9.** (a) <sup>1</sup>H NMR of C-NB-PS<sub>30</sub>-b-PtBA<sub>30</sub> before and after the deprotection. (b) <sup>1</sup>H NMR (solvent signals suppressed using DOSY) of C-NB-PS<sub>30</sub>-b-PtBA<sub>30</sub> before and after the deprotection.

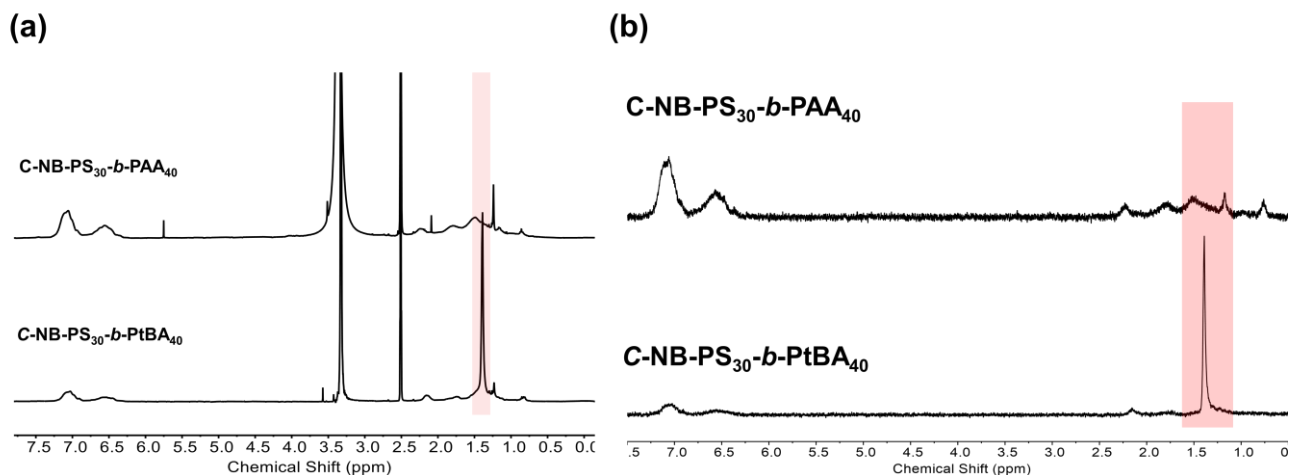


**Figure S10.** (a)  $^1\text{H}$  NMR of  $C\text{-NB-PS}_{30}\text{-}b\text{-PtBA}_{40}$  before and after the deprotection. (b)  $^1\text{H}$  NMR (solvent signals suppressed using DOSY) of  $C\text{-NB-PS}_{30}\text{-}b\text{-PtBA}_{40}$  before and after the deprotection.

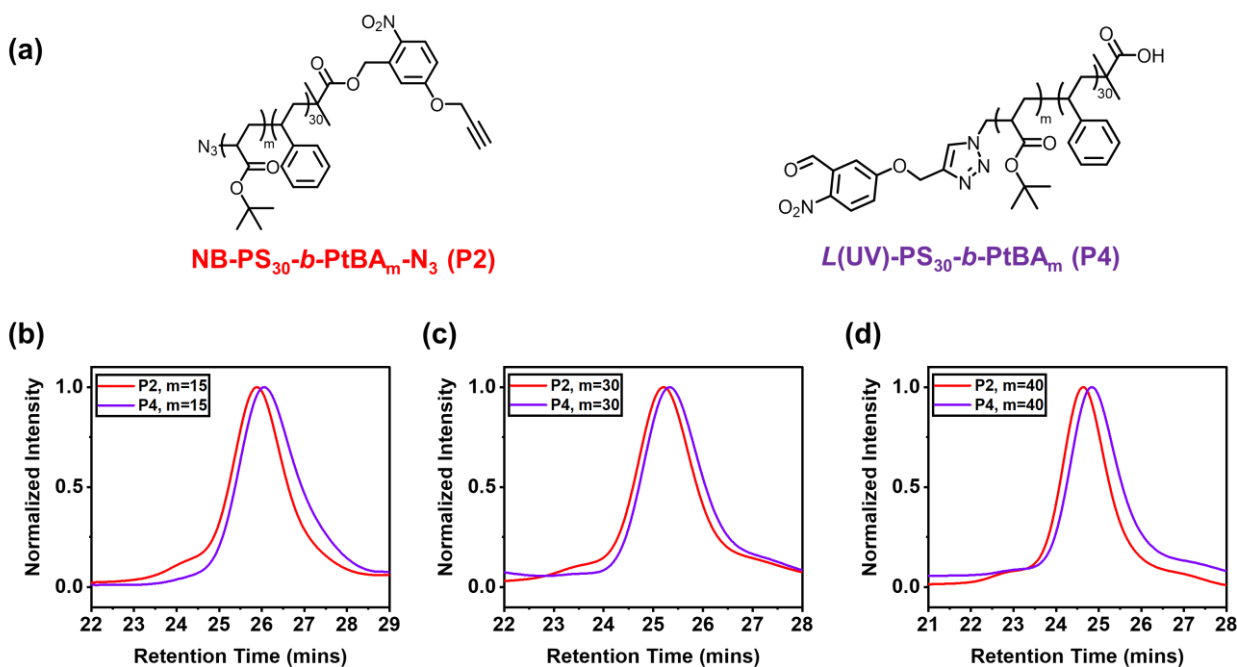


**Figure S11.** (a) Schematic illustration of the chemical structures of  $\text{NB-PS}_{30}\text{-}b\text{-PtBA}_m\text{-N}_3$  (P2) and  $L(\text{UV})\text{-NB-PS}_m\text{-}b\text{-PtBA}_m$  (P4); (b) SEC elugrams obtained from THF ( $40\text{ }^\circ\text{C}$  and  $1\text{ mL min}^{-1}$ ) of (b)  $\text{NB-PS}_{30}\text{-}b\text{-PtBA}_{15}\text{-N}_3$  and  $L(\text{UV})\text{-NB-PS}_m\text{-}b\text{-PtBA}_{15}$ , (c)  $\text{NB-PS}_{30}\text{-}b\text{-PtBA}_{30}\text{-N}_3$  and  $L(\text{UV})\text{-NB-PS}_m\text{-}b\text{-PtBA}_{30}$ , and (d)  $\text{NB-PS}_{30}\text{-}b\text{-PtBA}_{40}\text{-N}_3$  and  $L(\text{UV})\text{-NB-PS}_m\text{-}b\text{-PtBA}_{40}$ .

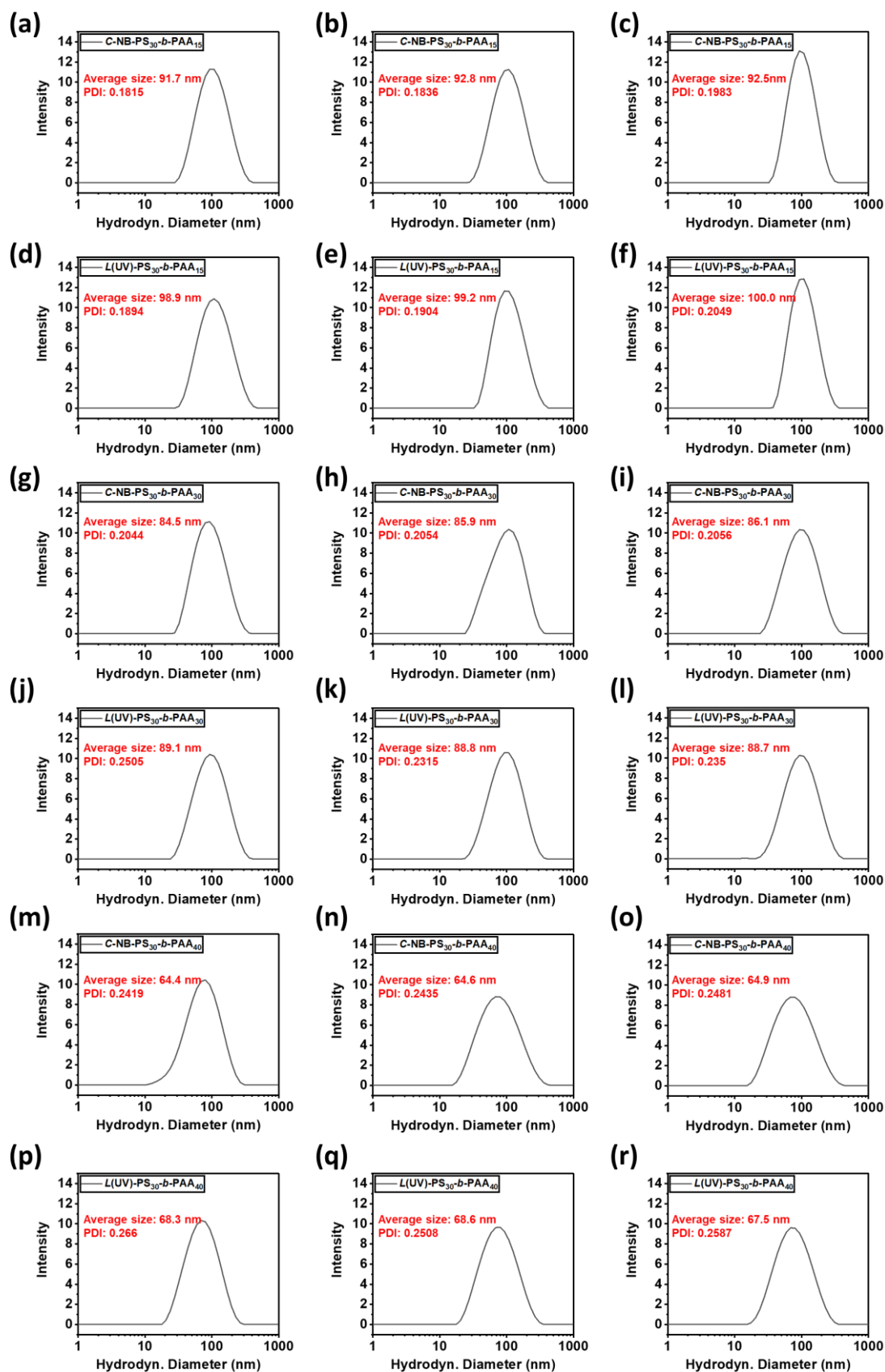


**Figure S12.** DLS measurements of the size distribution of (a)-(c) C-NB-PS<sub>30</sub>-b-PAA<sub>15</sub>, (d)-(f) L(UV)-PS<sub>30</sub>-b-PAA<sub>15</sub>, (g)-(i) C-NB-PS<sub>30</sub>-b-PAA<sub>30</sub>, (j)-(l) L(UV)-PS<sub>30</sub>-b-PAA<sub>30</sub>, (m)-(o) C-NB-PS<sub>30</sub>-b-PAA<sub>40</sub>, (p)-(r) L(UV)-PS<sub>30</sub>-b-PAA<sub>40</sub> assemblies in PBS with concentration at 0.2 mg/mL.

## S2. Drug Release Profile of Self-Assembled Polymer Nanoparticles

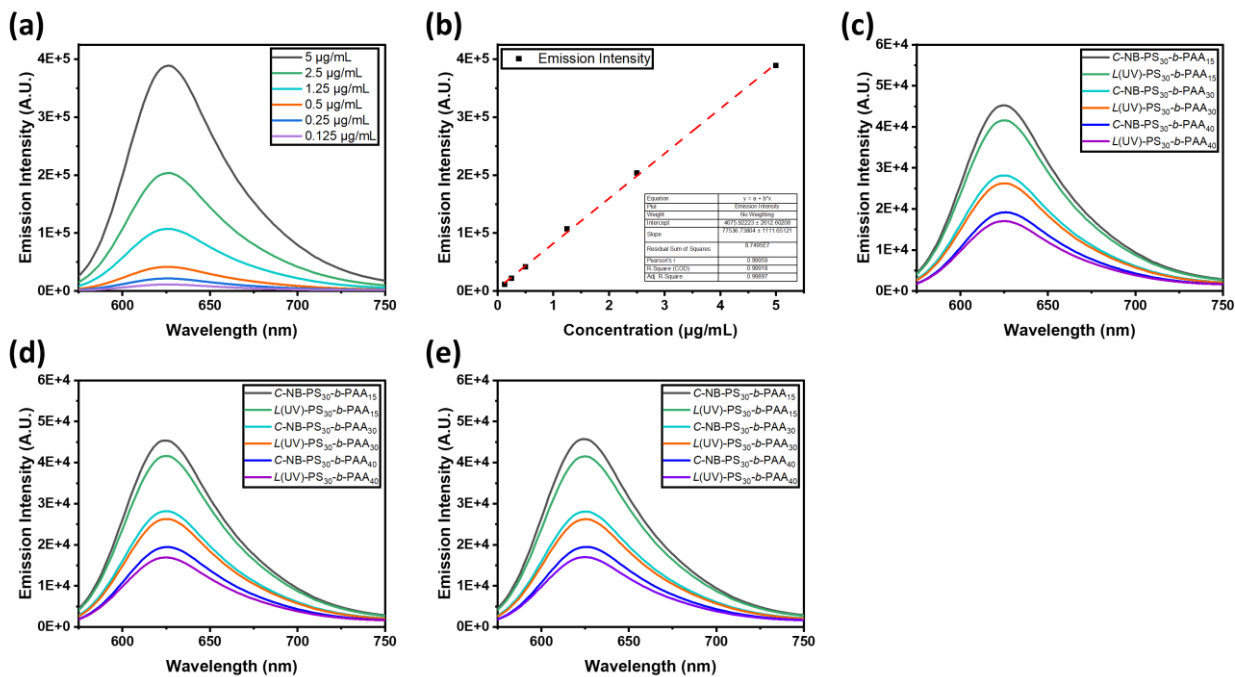


**Figure S13.** (a) Fluorescence emission spectra of Nile red at specific concentrations (5, 2.5, 1.25, 0.5, 0.25, 0.125  $\mu\text{g/mL}$ ) in DMF; (b) derived standard curve (reading at 625 nm) of Nile red in DMF; (c)-(f) Three trials of fluorescence emission spectra of Nile red in DMF after freeze-drying NR loaded polymer solutions for the calculation of encapsulation efficiency.

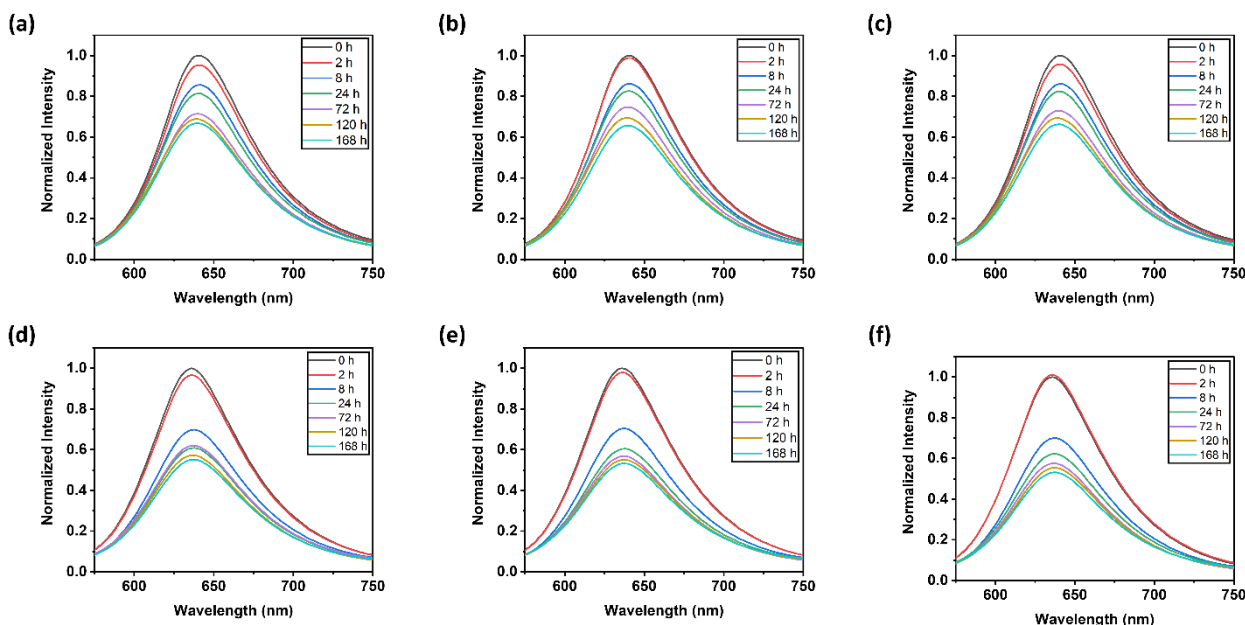


**Figure S14.** (a)-(c) Triplicate experiments of fluorescence emission spectra of Nile red incorporated into the *C-NB-PS<sub>30</sub>-b-PAA<sub>15</sub>* assemblies at various time points; (d)-(f) Triplicate experiments of fluorescence emission spectra of Nile red incorporated into the *L(UV)-PS<sub>30</sub>-b-PAA<sub>15</sub>* assemblies at various time points.

various time points.

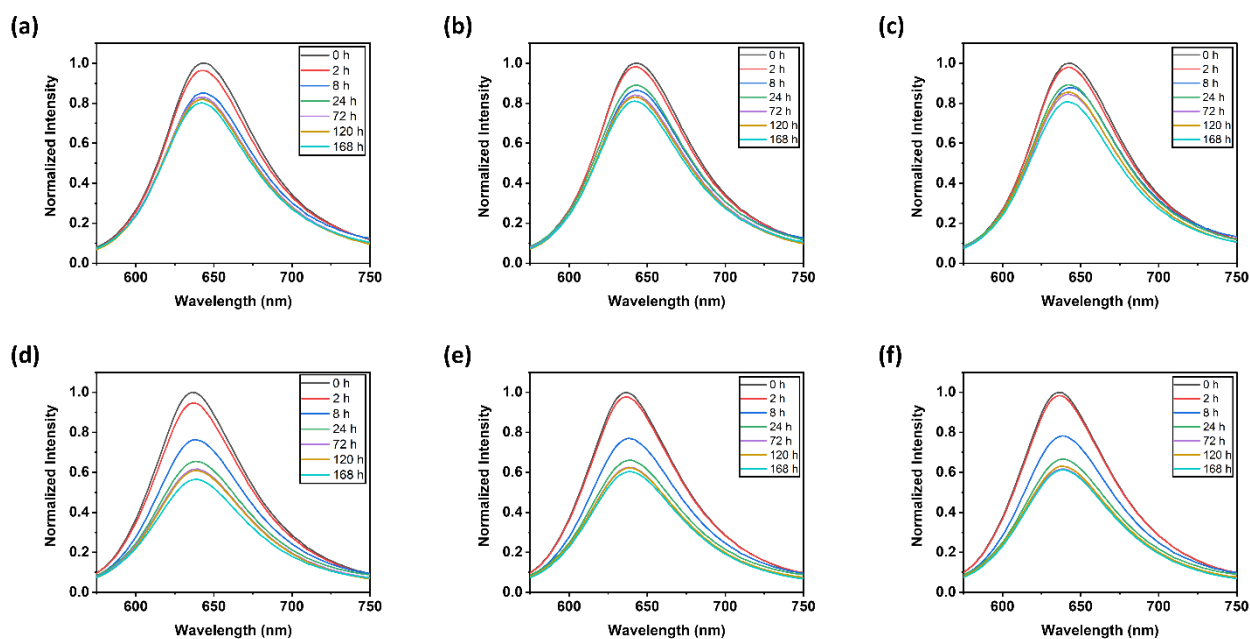


**Figure S15.** (a)-(c) Triplicate experiments of fluorescence emission spectra of Nile red incorporated into the *C*-NB-PS<sub>30</sub>-*b*-PAA<sub>30</sub> assemblies at various time points; (d)-(f) Triplicate experiments of fluorescence emission spectra of Nile red incorporated into the *L*(UV)-PS<sub>30</sub>-*b*-PAA<sub>30</sub> assemblies at various time points.

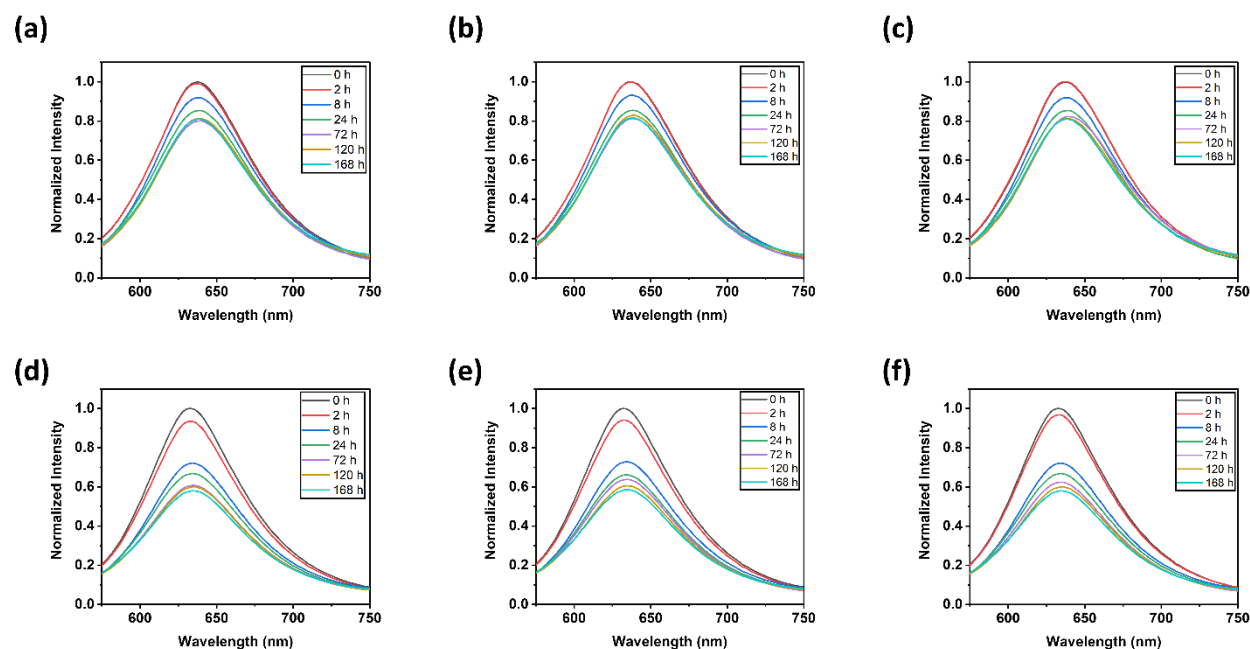


**Figure S16.** (a)-(c) Triplicate experiments of fluorescence emission spectra of Nile red incorporated into the *C*-NB-PS<sub>30</sub>-*b*-PAA<sub>40</sub> assemblies at various time points; (d)-(f) Triplicate experiments of fluorescence emission spectra of Nile red incorporated into the *L*(UV)-PS<sub>30</sub>-*b*-PAA<sub>40</sub> assemblies at various time points.

various time points.

### S3. EIS Experiment Set-up and Results

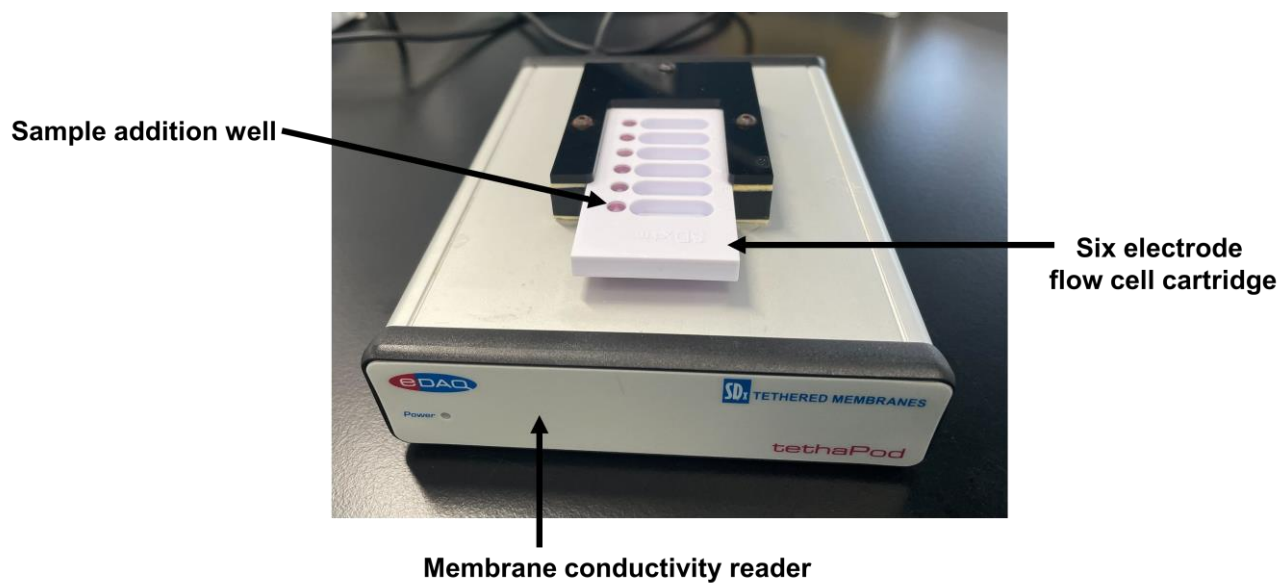


**Figure S17.** Schematic illustration of the experiment set up for the EIS to measure the interactions between polymer nanoparticles and model membranes.

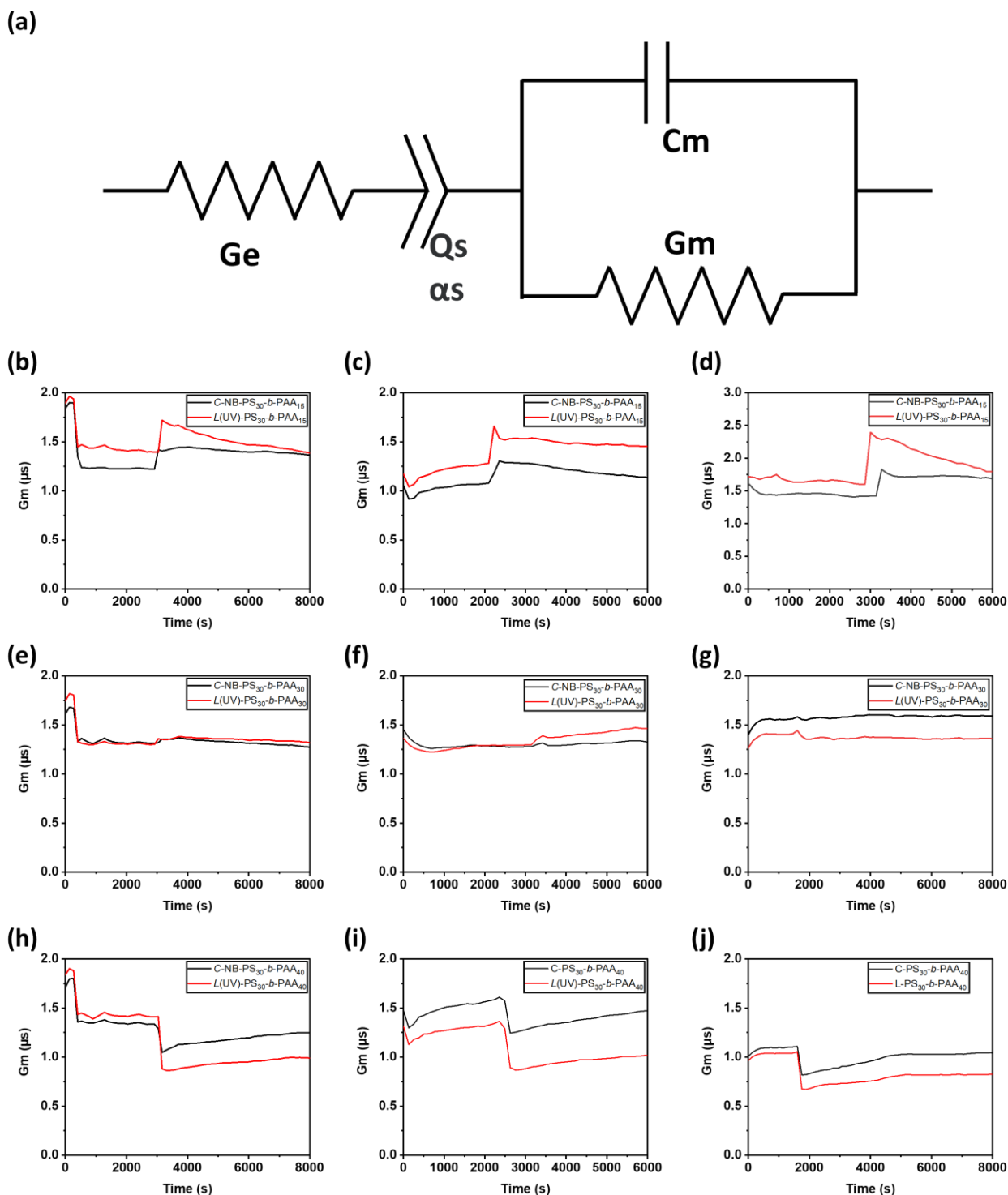


**Figure S18.** Electrical characteristics of the tethered lipid membrane bilayers (tBLM). (a) Equivalent circuit model used to analyse the electrical impedance spectroscopy (EIS) measurements of the tBLM, for the conductance of the solutions ( $G_m$ ) and the capacitance of the tBLM ( $C_m$ ); (b)-(d) Changes in the conductance of the solutions of tBLM after the addition of *C-NB-PS<sub>30</sub>-b-PAA<sub>15</sub>* and *L(UV)-PS<sub>30</sub>-b-PAA<sub>15</sub>* assemblies; (e)-(g) Changes in the conductance of the solutions of tBLM after the addition of *C-NB-PS<sub>30</sub>-b-PAA<sub>30</sub>* and *L(UV)-PS<sub>30</sub>-b-PAA<sub>30</sub>* assemblies; (h)-(j) Changes in the conductance of the solutions of tBLM after the addition of *C-NB-PS<sub>30</sub>-b-PAA<sub>40</sub>* and *L(UV)-PS<sub>30</sub>-b-PAA<sub>40</sub>* assemblies.

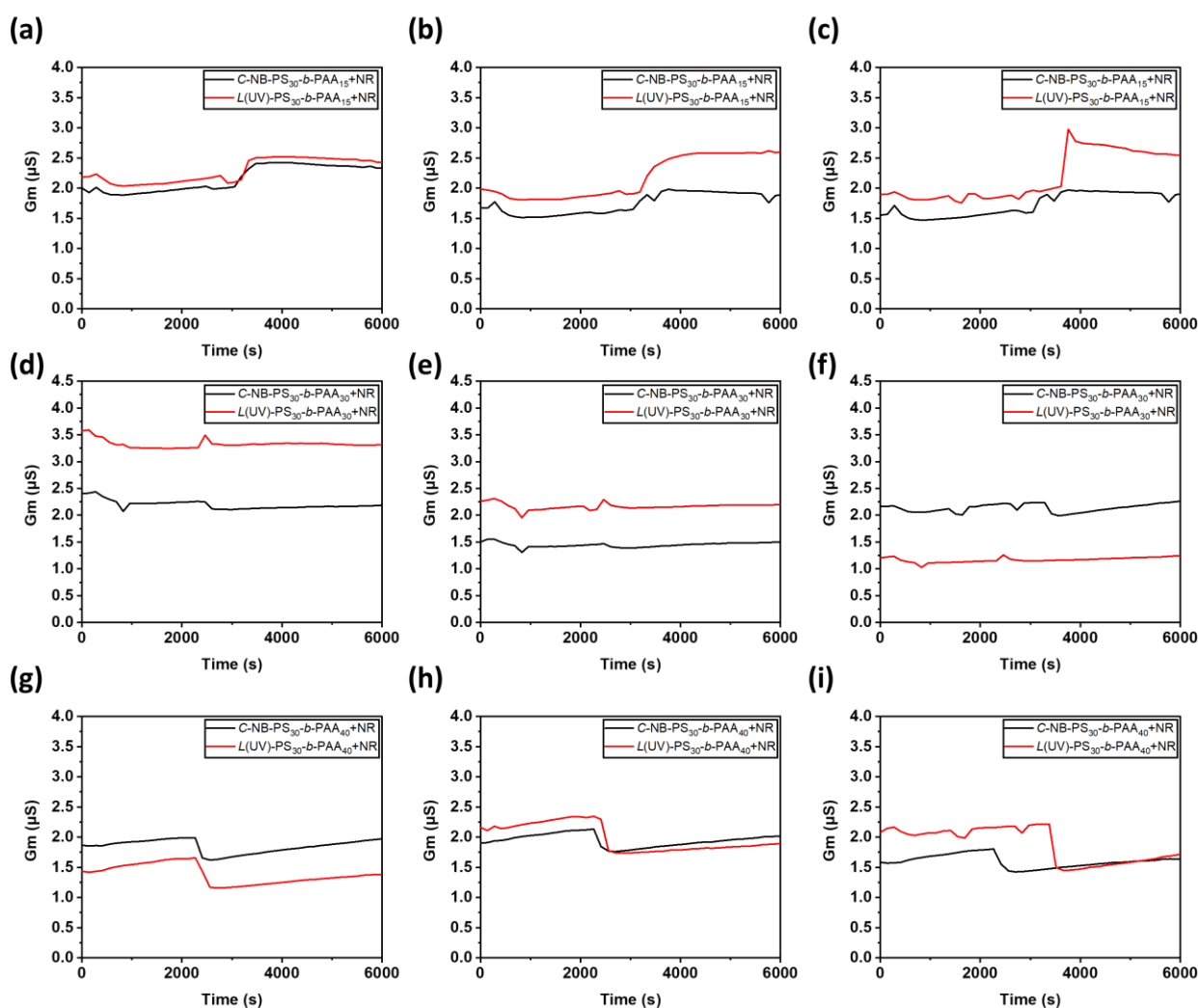


**Figure S19.** Electrical characteristics of the tethered lipid membrane bilayers (tBLM). (a)-(c) Changes in the conductance of the solutions of tBLM after the addition of NR loaded  $C\text{-NB-PS}_{30}\text{-}b\text{-PAA}_{15}$  and  $L(\text{UV})\text{-PS}_{30}\text{-}b\text{-PAA}_{15}$  assemblies; (e)-(g) Changes in the conductance of the solutions of tBLM after the addition of NR loaded  $C\text{-NB-PS}_{30}\text{-}b\text{-PAA}_{30}$  and  $L(\text{UV})\text{-PS}_{30}\text{-}b\text{-PAA}_{30}$  assemblies; (h)-(j) Changes in the conductance of the solutions of tBLM after the addition of NR loaded  $C\text{-NB-PS}_{30}\text{-}b\text{-PAA}_{40}$  and  $L(\text{UV})\text{-PS}_{30}\text{-}b\text{-PAA}_{40}$  assemblies.

## References

- 1 J.-M. Schumers, J.-F. Gohy and C.-A. Fustin, *Polym. Chem.*, 2010, **1**, 161–163.